

Bax is activated during rotavirus-induced apoptosis through the mitochondrial pathway.

Sandra Martin-Latil, Laurence Mousson, Arnaud Autret, Florence Colbère-Garapin, Bruno Blondel

▶ **To cite this version:**

Sandra Martin-Latil, Laurence Mousson, Arnaud Autret, Florence Colbère-Garapin, Bruno Blondel. Bax is activated during rotavirus-induced apoptosis through the mitochondrial pathway.. Journal of Virology, 2007, 81 (9), pp.4457-64. 10.1128/JVI.02344-06 . pasteur-00146502

HAL Id: pasteur-00146502
https://pasteur.hal.science/pasteur-00146502

Submitted on 16 Sep 2008

HAL is a multi-disciplinary open access archive for the deposit and dissemination of scientific research documents, whether they are published or not. The documents may come from teaching and research institutions in France or abroad, or from public or private research centers.

L'archive ouverte pluridisciplinaire **HAL**, est destinée au dépôt et à la diffusion de documents scientifiques de niveau recherche, publiés ou non, émanant des établissements d'enseignement et de recherche français ou étrangers, des laboratoires publics ou privés.

Bax is activated during rotavirus-induced apoptosis through the mitochondrial pathway

Sandra Martin-Latil*, Laurence Mousson, Arnaud Autret, Florence Colbère-Garapin, and Bruno Blondel

Unité de Biologie des Virus Entériques, Institut Pasteur, 25 rue du Docteur Roux, 75724 Paris cedex 15, France

*Corresponding author :

Dr. Sandra Martin-Latil, Unité de Biologie des Virus Entériques, Institut Pasteur, 28 rue du Docteur Roux, 75724 Paris cedex 15, France. Phone: (33) 1.40.61.35.90; Fax: (33) 1.40.61.34.21; E-mail: smartin@pasteur.fr

Running title: rotavirus induces Bax-dependent apoptosis

Word count abstract : 167

Word count manuscript without references, footnotes, figure legends : 4418

ABSTRACT

Rotaviruses are the leading cause of infantile viral gastroenteritis worldwide. Mature enterocytes of the small intestine infected by rotavirus undergo apoptosis and their replacement by less differentiated dividing cells probably leads to defective absorptive function of the intestinal epithelium, and this contributes to osmotic diarrhea and rotavirus pathogenesis.

Here, we show that the infection of MA104 cells by the simian rhesus rotavirus strain RRV induced caspase-3 activation, DNA fragmentation and cleavage of poly(ADP-ribose) polymerase (PARP); all three phenomena are features of apoptosis. RRV induced the release of cytochrome c from mitochondria to the cytosol indicating that the mitochondrial apoptotic pathway was activated. RRV infection of MA104 cells activated Bax, a proapoptotic member of the Bcl-2 family, as revealed by its conformational change. Most importantly, Bax-specific small interfering RNAs partially inhibited the cytochrome c release in RRV-infected cells. Thus, mitochondrial dysfunction induced by rotavirus is Bax-dependent. Apoptosis presumably leads to impaired intestinal functions, so our findings contribute to improve our understanding of rotavirus pathogenesis at the cellular level.

INTRODUCTION

Rotavirus is a nonenvelopped, double-stranded RNA virus belonging to the *Reoviridae* family. It is the major etiologic agent of severe gastroenteritis in children under 5 years of age and causes 600,000 deaths per year (40). Rotavirus infection is mainly restricted to the small intestinal villus epithelium, resulting in villus atrophy. Diarrhea associated with rotavirus is a multifactorial process: it involves dysfunctions of both nutrient digestion and enterocyte absorption at the top of villi, and the secretion of water and electrolytes (29, 32, 43). The defective absorptive function and the increased intestinal permeability may be a consequence of the replacement of rotavirus-infected mature enterocytes by less differentiated cells and this could contribute to rotavirus pathogenesis. In a murine model, rotavirus-infected enterocytes undergo apoptosis and are therefore lost (4). It is therefore likely that apoptosis makes a major contribution to diarrhea associated with rotavirus infection.

Cell death by apoptosis is part of the normal development and maintenance of homeostasis (51) but is also involved in pathological situations associated with infections (16, 45) and other (3) causes. Apoptosis is characterized by chromatin condensation, cell shrinkage, membrane bledding, and DNA fragmentation. It can be generally divided into two nonexclusive pathways, the death receptor pathway (extrinsic) and the mitochondrial pathway (intrinsic) (10, 13, 20). In the extrinsic pathway, stimulation of death receptors, such as Fas and TNF receptor 1, leads to formation of the death-inducing signaling complex (DISC) which allows the activation of caspase-8 and/or caspase-10, and then to that of downstream effector caspases, particularly caspase-3 (2, 34). The intrinsic pathway is initiated in response to diverse apoptotic stimuli and leads to the loss of mitochondrial transmembrane potential and the release of several pro-apoptotic proteins, including cytochrome c and Smac/Diablo, from the mitochondrial intermembrane space to the cytosol. Once released, cytochrome c

61 forms a complex with Apaf-1 and pro-caspase 9, resulting in activation of this initiator
62 caspase, and then of effector caspases (52). Smac/Diablo promotes caspase activation by
63 directly binding to and inhibiting the caspase inhibitors of the IAP family (50, 52). This
64 mitochondrial apoptotic pathway is tightly controlled by protein members of the Bcl-2 family.
65 Some, including Bcl-2 and Bcl-X_L, inhibit apoptosis, whereas others, including Bax and Bid,
66 induce apoptosis (9).
67 The extrinsic and intrinsic pathways may cross-talk through the pro-apoptotic protein Bid.
68 Indeed, caspase-8 can cleave Bid to generate a truncated form, tBid that targets mitochondria
69 and activates the pro-apoptotic protein Bax (26, 27, 30).
70 There have been very few studies of rotavirus-induced apoptosis in primate cells *in vitro*. An
71 early study in human carcinoma HT29 cells indicated that rotavirus induced peripheral
72 condensation of the chromatin and fragmentation of the nuclei, suggesting that apoptosis was
73 induced in infected cells (47). A more recent study in fully differentiated Caco-2 cells
74 indicated that rotavirus induced apoptosis in these cells, and did so through the mitochondrial
75 pathway (7). However, the precise signaling pathways leading to mitochondrial dysfunction
76 following rotavirus infection have not been investigated.
77 Here, we studied apoptosis induced by the Rhesus Rotavirus (RRV) strain in the monkey
78 kidney MA104 cells, the cellular model in which the rotavirus cycle has been best
79 characterized. We first confirmed that RRV-induced apoptosis in this model occurs through
80 the mitochondrial pathway as observed in Caco-2 cells. We then investigated the cascade of
81 events related to mitochondrial dysfunction. We report here that mitochondrial apoptotic
82 pathway in RRV-infected MA104 cells is Bax-dependent. It is, to our knowledge, the first
83 demonstration of Bax-dependent apoptosis in rotavirus-infected cells.

MATERIALS AND METHODS

Materials – Chemicals

Protein G (P3296), Staurosporine (S4400) and mouse anti-tubulin antibody (T5168) were obtained from Sigma-Aldricht. CompleteTM protease inhibitor mixture was obtained from Roche Applied Science. z-VAD-fmk (627610), z-DEVD-fmk (264155) and z-LEHD-fmk (218761) were purchased from Calbiochem. Mouse anti-CoxIV (A21347) antibody was purchased from Molecular Probes. Mouse anti-Bcl-2 (sc-509) and anti-Bax (clone 6A7, sc-23959) antibodies were purchased from Santa Cruz Biotechnology. Rabbit anti-Bax antibody (NT 06-499) and mouse anti-cytochrome c antibody (556433) were obtained from Upstate and BD Pharmingen, respectively. Rabbit anti-Smac/Diablo (2409) was purchased from ProSci incorporated. Anti-mouse (NA9310V) and anti-rabbit (NA9340V) HRP-conjugated secondary antibodies were obtained from Amersham Biosciences. Goat anti-Bid antibody (AF860) and donkey anti-goat (HAF109) HRP-conjugated antibody were purchased from Research & Diagnostic. Mouse anti-PARP antibody (clone C-2-10) was obtained from Biomol. Mouse anti-Caspase-3 (9668) and anti-caspase-8 (9746) antibodies, and Bax (6321) and non-targeted control (6201) siRNAs were purchased from Cell Signaling.

Cells and Virus

The monkey kidney MA104 cell line (MA104 cells) was cultured in minimum Eagle's medium (MEM) supplemented with 10% fetal bovine serum (FBS), 2 mM glutamine and 0.1 mM non-essential amino acids, in a 5% CO2 incubator. The rotavirus RRV strain was kindly provided by Didier Poncet (Gif-sur-Yvette, France). Virus stocks were generated in MA104 cells in a serum-free culture medium supplemented with trypsin (0.5 μg/ml). Viruses were activated by treatment with trypsin at 37°C for 30 min, and MA104 cell monolayers were

infected at a multiplicity of infection (m.o.i.) of 0.002 plaque-forming units/cell. After 1 h of adsorption at 37°C, the inoculum was removed and the infected cells were incubated in serum-free medium containing trypsin. When cytopathic effects were complete, the cultures were frozen and then thawed, and the cell debris was removed by centrifugation.

To infect MA104 cells, RRV was activated in serum-free medium with 0.5 µg/ml trypsin. Cells were washed twice in serum-free medium and then infected at an m.o.i of 10. The inoculum was removed 1 h later and replaced with medium containing 10% FBS. This time was defined as 0 h post-infection for all experiments.

Assessment of apoptosis by flow cytometry

The percentages of cells that were apoptotic was determined by flow cytofluorimetric analysis of aliquots of 2 x 10^6 cells incubated with acridine orange (AO), a metachromatic nuclear dye (λEx_{max}: 500 nm, λEm_{max}: 526 nm), for 15 min at 37°C. AO fluorescence was measured with a FACScan machine (Becton Dickinson). Two populations of cells were separated, one consisting of the living cells characterized by a bright fluorescence labeling, and the second being apoptotic cells with a characteristic distinct pattern of reduced fluorescence intensity (12). We analyzed at least 10,000 cells for each sample. Data were analyzed with Cellquest software (Becton Dickinson).

Quantification of oligonucleosomal DNA fragmentation

DNA fragmentation was assayed using a cell death detection ELISA kit (Roche Applied Science) with RRV-infected MA104 cells plated in 6-well culture dishes according to the manufacturer's instructions; the test measures the cytosolic histone-associated mono- and oligonucleosome fragments. The concentration of nucleosomal fragments in cytosolic fractions was determined by a sandwich enzyme-linked immunosorbent assay, using histone-

specific antibodies preadsorbed onto microtiter plates and peroxidase-conjugated antibodies against DNA. Peroxidase activity was measured photometrically at 405 nm. The experiments were run in triplicate.

Detection of active caspase-8

Caspase-8 activation was detected using a carboxyfluorescein FLICA apoptosis detection kit (Immunochemistry Technologies, LLC) according to manufacturer's protocol. This assay is based on a fluorescein-labeled inhibitor (FAM-LETD-fmk) that binds specifically to active caspase-8. Apoptotic cells containing active caspase-8 were detected with a FACScan (Becton Dickinson) machine. We analyzed at least 10,000 cells for each sample. Data were analyzed with Cellquest software (Becton Dickinson).

Transfection of small interfering RNA (siRNA)

RNA interference was used to silence Bax gene expression in MA104 cells. Cells were plated in 6-well culture dishes with complete medium and allowed to grow for 24 h, so as to reach 50–80% confluence. The cells were then transfected with siRNA (6321, Cell Signaling) targing Bax mRNA. An irrelevant siRNA (6201, Cell Signaling) that does not lead to the specific degradation of any cellular mRNA was used as a negative control. A mixture of OptiMEM medium and LipofectAMINE was incubated for 10 min at room temperature and was then incubated with siRNA (25 nM) for 20 min at room temperature to allow complex formation. This siRNA mixture was then added to each well following the manufacturer's suggested protocol. Twenty-four hours after transfection, the medium was changed and cells were infected with the virus 24 h later. Gene silencing was verified by testing for proteins by immunoblot analysis after transient transfection of MA104 cells with siRNA.

Whole cell extracts

Approximately 5.10^6 cells were collected and washed with PBS, then resuspended in lysis buffer (20 mM Tris pH 7.5, 135 mM NaCl, 2 mM EDTA, 1% Triton-X100, 10% glycerol) supplemented with a protease inhibitor mixture (Roche). The cells were homogenized on ice using dounce homogenizer and incubated for 10 min at 4°C in the lysis buffer. The lysates were clarified by centrifugation for 10 min at 1200 g. The supernatant was collected as the whole cell extract.

Subcellular fractionation

A subcellular proteome extraction kit (Calbiochem) was used to isolate cytosol and heavy membrane fractions of MA104 cells according to the manufacturer's instructions. Cells (5.10^6) were harvested, pelleted, washed twice, resuspended in the ice-cold Extraction I buffer containing a protease inhibitor mixture and incubated for 10 min at 4°C with gentle agitation. The suspension was centrifuged at 1000 g at 4°C for 10 min. The supernatant was used as the cytosol fraction. The pellet was resuspended in the ice-cold Extraction II buffer containing a protease inhibitor mixture and incubated for 30 min at 4°C with gentle agitation. It was then centrifuged at 6000 g for 10 min at 4°C, and the supernatant was used as the heavy membrane fraction.

Detection of Bax conformation change by immunoprecipitation

Cells were harvested, washed in PBS and suspended in lysis buffer (10 mM hepes pH 7.4, 150 mM NaCl, 1% Chaps) containing a mixture of protease inhibitors. The zwitterionic detergent Chaps was used because it does not affect Bax conformation (18). Cells were homogenized on ice with dounce homogenizer, incubated for 2 h in the lysis buffer and centrifuged for 30 min at 14000 g. The resulting supernatant was incubated overnight at 4°C

184 with 20 µl of protein G and 2 µg of the anti-Bax antibody (6A7). The immunoprecipitates
185 were collected by centrifugation at 14000 g (4°C, 5 min). The pellets were washed with
186 immunoprecipitation buffer and suspended in 50 µl of Laemmli's buffer containing reducing
187 agent (Invitrogen).
188
189 **Western-blot analysis**
190 Protein concentrations were determined by using a Bio-Rad protein assay kit (Bio-Rad,
191 Richmond, CA). Samples of equal protein content were resuspended in Laemmli's
192 electrophoresis sample buffer containing reducing agent, denatured by boiling for 5 min,
193 subjected to SDS-PAGE (10-20% Tricine gels; Novex) and transferred to nitrocellulose
194 membranes (Amersham Biosciences). Nonspecific sites were blocked by incubating the
195 membranes for 1 h at room temperature with 5% nonfat milk and 0.1% Tween 20 in
196 Phosphate-Buffered Saline (PBST, pH 7.4), and the membranes were incubated overnight at
197 4°C or 2 h at room temperature with the primary antibody. Membranes were then washed in
198 PBST and treated with appropriate horse-radish peroxidase-conjugated secondary antibody
199 for 1 h at room temperature. The immunoblots were washed in PBST and developed using an
200 enhanced chemiluminescence detection kit (Amersham Biosciences). Anti-tubulin and Cox
201 IV antibodies were used to verify equal protein loading.
202
203 **Statistical Analysis**
204 Data are expressed as means ± SEM of three independent experiments. Student's test was
205 used to compare experimental conditions and controls. A value of $P<0.05$ was considered
206 significant.
207

RESULTS

RRV infection induces apoptosis in MA104 cells through the mitochondrial pathway.

Apoptosis induced by RRV in MA104 cells was investigated by following the kinetics of DNA fragmentation with the Cell Death ELISA kit (Roche) (Fig. 1A). Early p.i. (until 8h p.i.), DNA fragmentation was not significantly different in infected and uninfected cells. Enrichment of nucleosomal DNA fragments started by 12 h p.i. and increased until 20 h p.i. DNA fragmentation 20 h p.i. was 3-to 4-fold that of mock-infected cells and similar to that observed after 14 h of treatment with staurosporine, used as positive control for DNA fragmentation. These results confirm that rotavirus induced apoptosis in MA104 cells.

We then looked for activation of caspase-3, the central executioner in the apoptotic program, in RRV-infected MA104 cells. Cleavage of 32 kDa procaspase-3 revealed by the detection, in a whole cell lysate, of its 19 kDa cleavage product was substantial at about 14 h p.i. (Fig. 1B). To confirm the activation of caspase-3 in RRV-infected MA104 cells, we investigated the processing of one of its characteristic substrates, the poly(ADP-ribose) polymerase (PARP) (Fig. 1B). The amount of full-length PARP in a whole lysate of RRV-infected MA104 cells declined from 14 to 22 h p.i., thus paralleling the pattern of caspase-3 activation. These results show that rotavirus induced caspase executioner activation in MA104 cells. Furthermore, the peak of caspase-3 activation coincided with that of virus production during a single-cycle infection in the same experimental conditions (data not shown).

To assess the role of caspases in cell death resulting from RRV infection, infected cells were treated with a broad-spectrum caspase inhibitor, z-VAD-fmk (10 μM, Calbiochem). The roles of caspase-9 and caspase-3 were investigated with specific inhibitors, z-LEHD-fmk (10 μM, Calbiochem) and z-DEVD-fmk (10 μM, Calbiochem), respectively. Apoptosis was analyzed 14 h p.i., by measuring chromatin condensation and fragmentation by flow cytometry after

Acridine Orange (AO) staining (Fig. 1C). The three caspase inhibitors significantly reduced the percentage of apoptotic cells following RRV infection with respect to that in their untreated counterparts. (The same level of apoptosis inhibition was observed with z-VAD-fmk at a concentration of 100 μM, data not shown). These results indicate that caspases are, at least partly, involved in RRV-induced apoptosis. Furthermore, the decrease in apoptosis in cells treated with the caspase 9 inhibitor seems to indicate that the mitochondrial pathway is activated in RRV-infected cells.

To confirm that the mitochondrial pathway is activated during RRV infection in MA104 cells, we investigated the kinetics of cytochrome c and Smac/Diablo efflux from mitochondria into the cytosol. Infected cells were fractionated to separate the cytosolic fraction from the heavy membrane fraction containing mitochondria, at various times after infection, and the fractions were studied by western blotting (Fig. 2). Cytochrome c and Smac/Diablo were detected in the cytoplasm of infected MA104 cells from 9 h p.i. and 12 h p.i., respectively: they increased in amount in the the cytosol thereafter until the last time point investigated (18 h p.i.) whereas they decreased in amount in the heavy membrane fraction. These findings indicate that rotavirus causes the release of cytochrome c and Smac/Diablo into the cytosol in MA104 cells, consistent with apoptotic mitochondrial dysfunction.

RRV-induced mitochondrial apoptotic pathway is caspases- and Bid-independent.

We then looked for upstream signals that could trigger the activation of the mitochondrial apoptotic pathway following RRV infection. This pathway can be activated by the BH3-only protein Bid following its cleavage by caspase-8 (26, 30). First, the kinetics of the processing of procaspase-8 was analyzed in RRV-infected MA104 cells, by immunoblotting (Fig. 3A). The amounts of procaspase-8 decreased from 14 h p.i., relative to those in mock-infected cells, suggesting caspase-8 activation. Caspase-8 activation was confirmed at 14 h p.i. by flow

cytometry with a FLICA apoptosis detection kit, based on the specific binding of a fluorescein-labeled inhibitor (FAM-LETD-fmk, Immunochemistry Technologies, LLC) to active caspase (Fig 3B). The kinetics of Bid processing was then analyzed in RRV-infected MA104 cells, by immunoblotting (Fig. 3A). The amounts of Bid and procaspase-8, decreased with respect to those in mock-infected cells, suggesting a cleavage of Bid mediated by activated caspase-8.

To determine whether caspase-8 and Bid were required for engaging mitochondrial pathway of apoptosis, we assessed cytochrome c release in the presence of the broad-spectrum caspase inhibitor, z-VAD-fmk. The release of cytochrome c from the mitochondria into the cytosol in RV-infected MA104 cells (14 h p.i.) was analyzed by western blotting following subcellular fractionation (Fig. 4). As expected, cleavage of both Bid and PARP were inhibited in the presence of the caspase inhibitor (Fig. 4A). In contrast, z-VAD-fmk was unable to prevent cytochrome c release (Fig. 4B), suggesting that mitochondrial dysfunction in RRV-infected MA104 cells is induced by a caspase- and Bid-independent mechanism. Thus, caspases seem to be involved in RRV-induced apoptosis at a position in the pathway downstream from the mitochondrial dysfunction.

Bax is activated during RRV infection by a caspase independent pathway.

The proapoptotic Bcl-2 family protein Bax is a pivotal regulator of cytochrome c release from mitochondria to the cytosol (1, 38, 53). In healthy cells, most Bax is in the cytoplasm and in an inactive form. Bax-mediated cell death occurs through a conformational change and its translocation to the mitochondrial outer membrane, resulting in the loss of mitochondrial membrane potential and the release of proapoptogenic factors including cytochrome c (18, 33, 54). We investigated kinetics of the conformational change of Bax in RRV-infected cells. Total cell lysates were prepared at the indicated times post-infection (p.i) (Fig. 5A) in a lysis

buffer (containing Chaps) that did not affect Bax conformation. Bax was then immunoprecipitated with an anti-Bax antibody (6A7) specific for the active conformation of Bax (18, 19) and visualized by western blotting (Fig. 5A). In mock-infected cells, no activated Bax was detected in the immunoprecipitates. From 12 h p.i, Bax was precipitated by antibody 6A7, indicating that RRV infection induced the conformational change of Bax as observed in STS-treated cells used as positive control (data not shown). Thus, rotavirus infection triggers a conformational change in Bax in MA104 cells. Furthermore, we showed that Bax activation still occured in the presence of the broad-spectrum caspase inhibitor, z-VAD-fmk (100 μM, Calbiochem) (Fig. 5B), indicating that Bax activation during RRV infection is caspase independent.

MA104 cell infection by RRV increases the Bax/Bcl-2 ratio.

The Bcl-2-family, obviously, includes the antiapoptotic protein Bcl-2, which converges on mitochondria and competes with proapoptotic Bax to regulate the release of cytochrome c in response to apoptotic signal (1, 15, 44). As the ratio of pro- and anti-apoptotic proteins determines, at least in part, the susceptibility of cells to the death signal (38), we studied the time-dependent effects of RRV infection on Bax and Bcl-2 abundance in MA104 cells (Fig 5C). The amount of Bcl-2 decreased as the viral infection proceeded, whereas the total amount of Bax was unaffected. Thus rotavirus infection increased the Bax/Bcl-2 ratio and this could contribute to the mitochondrial apoptotic pathway by increasing the amount of free Bax thereby allowing its activation.

RRV-induced mitochondrial apoptotic pathway is Bax-dependent.

These various findings seem to indicate that RRV induces Bax-mediated apoptosis in MA104 cells. To assess the requirement for Bax in RRV-induced mitochondrial dysfunction, MA104

cells were transiently transfected with specific small interfering RNA (siRNA) to knock down Bax expression. Western blot analysis of MA104 cells transfected with the Bax siRNA (Cell Signaling) and with the irrelevant control siRNA (Cell Signaling) confirmed that the specific siRNA reduced significantly the abundance of Bax (50 %) (Fig 6A). We analyzed cytochrome c release 14 h after infection of MA104 cells previously transfected with siRNA. Bax siRNA partially inhibited cytochrome c release (52 %) in RRV-infected cells whereas the irrelevant control siRNA had no effect. Furthermore, a much larger proportion of cytochrome c remained in the membrane fraction containing mitochondria from RRV-infected cells treated with Bax siRNA than from those treated with the irrelevant control (Fig 6B). We also investigated RRV-induced apoptosis in MA104 cells, previously transfected with siRNA. The fraction of apoptotic cells analyzed at 14 h p.i., by flow cytometry after Acridine Orange (AO) staining, decreased in cells with reduced Bax expression (Fig. 6C). These results demonstrate that Bax plays a key role in rotavirus-induced mitochondrial pathway of apoptosis.

DISCUSSION

The pathophysiological mechanisms behind rotavirus-induced diarrhea have not been completely described. In mice, apoptosis may be associated with functional changes during rotavirus infection, particularly the modification of digestion and absorption functions. Evidence for apoptosis has been reported in intestinal cell lines following rotavirus infection *in vitro* (7, 47). However, the precise cellular and molecular mechanisms underlying rotavirus-induced apoptosis have not been defined. Here, we investigated the apoptosis induced by the RRV strain in MA104 cells, a monkey kidney epithelial cell line in which the rotavirus cycle has been best characterized.

We showed that several hallmarks of apoptosis, notably DNA fragmentation, caspase-3 activation and PARP cleavage, were detected following RRV infection of MA104 cells. DNA fragmentation was not observed in a previous study (6) in the same RRV-infected cells, probably because of differences in the sensitivity of the tests used. Moreover, we report the release of cytochrome c and Smac/DIABLO from mitochondria into the cytosol, implicating mitochondrial dysfunction in the apoptotic pathway. Cytochrome c release is known to be the pro-apoptotic signal causing the autocatalytic activation of procaspase-9 that triggers caspase-3 cleavage. We showed that specific inhibition of either caspase-3 or caspase-9 reduced the percentage of apoptotic cells following RRV infection. Thus, RRV-induced apoptosis is, at least partly, dependent on caspase activation. It is also possible that Smac/Diablo is associated with RRV-induced apoptosis through its action on cellular inhibitors of apoptosis proteins (IAPs), as observed notably during reovirus-induced apoptosis (22).

We then investigated events upstream from RRV-induced mitochondrial dysfunction. We focused on the Bcl-2 family proteins because they are central regulators of the mitochondrial apoptotic pathway (1, 15, 35, 44) and have been implicated in various models of virus-induced apoptosis (28, 36). Bax, one of the pro-apoptotic Bcl-2 family proteins, is the most downstream activator molecule known of cytochrome c release machinery (42). We showed that Bax is activated following RRV infection in MA104 cells: we detected its conformational modification involving the exposure of its N-terminal extremity required for insertion into mitochondrial membranes (18, 33). Once integrated into the outer mitochondrial membrane, Bax can trigger cytochrome c release leading to the activation of the effector caspase-3 and apoptotic cell death (11, 14, 23, 53). Our analysis of RRV-infected MA104 cells by using siRNA-mediated gene silencing indicates, for the first time, that the apoptotic mitochondrial pathway is activated through a Bax-dependent mechanism.

357 The inhibition of the prosurvival function of Bcl-2 is essential for the activation of Bax
358 because Bcl-2 can compete with Bax to regulate the release of cytochrome c (1, 15, 44). The
359 amount of antiapoptotic Bcl-2 protein decreased in RRV-infected cells without any change in
360 the amount of Bax. This results in an increase in the Bax/Bcl-2 ratio in RRV-infected cells
361 that could favor an increase in free Bax. Thus, one mechanism by which rotavirus may
362 contribute to Bax activation is by decreasing the number of Bax/Bcl-2 complexes at the
363 mitochondrial membrane.
364 Activated BH3-only proteins such as Bid can suppress the capacity of Bcl-2 to inhibit
365 apoptosis by interacting with it to displace and subsequently activate Bax (24, 25). Bid can be
366 activated by caspase-8, resulting in Bax activation and release of cytochrome c (23). We
367 showed that Bid processing was inhibited by the broad caspase inhibitor z-VAD-fmk in RRV-
368 infected cells; therefore rotavirus infection causes caspase-8 activation leading to Bid
369 activation. However, the inhibitor did not inhibit Bax activation and cytochrome c release,
370 suggesting that caspases and Bid do not play a crucial role in the Bax-dependent cytochrome
371 c release pathway during RRV infection. Thus, caspases seem to be involved in RRV-induced
372 apoptosis at a position in the pathway downstream from the mitochondrial dysfunction.
373 Several mechanisms for promoting Bax activation and mitochondrial dysfunction have been
374 described. These mechanisms include a signal transduction cascade involving mitogen-
375 activated protein kinases (MAPK) such as c-jun N-terminal protein kinase (JNK) and p38, as
376 described in other models (21, 49). The regulation of mitochondrial dysfunction by JNK
377 following virus infection was first demonstrated in reovirus-infected cells (8). Coulson *et al.*
378 (17) recently showed that JNK and p38, are activated by rotavirus infection in MA104 cells.
379 However the involvement of MAPK activation in Bax-dependent mitochondrial dysfunction
380 has not yet been demonstrated in rotavirus-infected cells.

Rotavirus infection of cultured cells induces a progressive rise in the cytosolic Ca^{2+} concentration (5, 31, 46, 48). This increase may be involved in rotavirus-induced apoptosis, and indeed, the intracellular calcium ion chelator BAPTA-AM partially inhibits apoptosis (7). The rise in cytosolic Ca^{2+} concentration in rotavirus-infected cells results from a progressive increase in plasma membrane permeability to Ca^{2+} and a depletion of endoplasmic reticulum (ER) pools. Xu et al. showed that rotavirus infection leads to ER stress (55). This stress and ER Ca^{2+} depletion may lead to Bax activation (39). It would be valuable to determine in future studies whether rotavirus induces apoptosis by inducing both ER stress and ER Ca^{2+} depletion leading to mitochondrial dysfunction. Several anti- and pro-apoptotic members of the Bcl-2 family have been found, in addition to their mitochondrial localization, to be associated to the ER and have been implicated in controlling apoptosis by affecting cellular Ca^{2+} homeostasis (37, 39, 41). As demonstrated in this study, Bax is involved in mitochondrial dysfunction in RRV infected-cells, but it could also be involved in ER Ca^{2+} release and thus amplify the apoptotic signal in RRV-infected cells. It would therefore be interesting to investigate whether Bax plays a role in ER Ca^{2+} release.

Apoptosis of mature rotavirus-infected enterocytes induces the replacement of these cells by less differentiated dividing cells. This event may well be the cause of the defective absorptive functions of the intestinal epithelial and consequently diarrhea associated with rotavirus pathogenesis (4). Thus, the identification of the apoptotic signaling pathways in RRV-infected cells would improve our understanding of the mechanisms by which rotavirus infection causes functional alterations. Our demonstration of the activation of Bax during rotavirus infection and its involvement in mitochondrial apoptotic pathway provide new insights concerning rotavirus-induced pathogenesis.

ACKNOWLEDGEMENTS

We thank Didier Poncet (Gif-sur-Yvette, France) for the gift of MA104 cells and the rotavirus RRV strain. We thank Isabelle Pelletier and Aure Saulnier for their help. This work was supported by the Institut Pasteur, Danone Research Centre Daniel Carasso and the Ministère de l'Education Nationale, de la Recherche et de la Technologie.

REFERENCES

1. **Adams, J. M., and S. Cory.** 2001. Life-or-death decisions by the Bcl-2 protein family. Trends Biochem Sci **26:**61-6.
2. **Ashkenazi, A., and V. M. Dixit.** 1998. Death receptors: signaling and modulation. Science **281:**1305-8.
3. **Blomgren, K., C. Zhu, X. Wang, J. O. Karlsson, A. L. Leverin, B. A. Bahr, C. Mallard, and H. Hagberg.** 2001. Synergistic activation of caspase-3 by m-calpain after neonatal hypoxia-ischemia: a mechanism of "pathological apoptosis"? J Biol Chem **276:**10191-8.
4. **Boshuizen, J. A., J. H. Reimerink, A. M. Korteland-van Male, V. J. van Ham, M. P. Koopmans, H. A. Buller, J. Dekker, and A. W. Einerhand.** 2003. Changes in small intestinal homeostasis, morphology, and gene expression during rotavirus infection of infant mice. J Virol **77:**13005-16.
5. **Brunet, J. P., J. Cotte-Laffitte, C. Linxe, A. M. Quero, M. Geniteau-Legendre, and A. Servin.** 2000. Rotavirus infection induces an increase in intracellular calcium concentration in human intestinal epithelial cells: role in microvillar actin alteration. J Virol **74:**2323-32.

6. **Castilho, J. G., M. V. Botelho, F. Lauretti, N. Taniwaki, R. E. Linhares, and C. Nozawa.** 2004. The in vitro cytopathology of a porcine and the simian (SA-11) strains of rotavirus. Mem Inst Oswaldo Cruz **99:**313-7.

7. **Chaibi, C., J. Cotte-Laffitte, C. Sandre, A. Esclatine, A. L. Servin, A. M. Quero, and M. Geniteau-Legendre.** 2005. Rotavirus induces apoptosis in fully differentiated human intestinal Caco-2 cells. Virology **332:**480-90.

8. **Clarke, P., S. M. Meintzer, Y. Wang, L. A. Moffitt, S. M. Richardson-Burns, G. L. Johnson, and K. L. Tyler.** 2004. JNK regulates the release of proapoptotic mitochondrial factors in reovirus-infected cells. J Virol **78:**13132-8.

9. **Cory, S., and J. M. Adams.** 2002. The Bcl2 family: regulators of the cellular life-or-death switch. Nat Rev Cancer **2:**647-56.

10. **Danial, N. N., and S. J. Korsmeyer.** 2004. Cell death: critical control points. Cell **116:**205-19.

11. **Desagher, S., A. Osen-Sand, A. Nichols, R. Eskes, S. Montessuit, S. Lauper, K. Maundrell, B. Antonsson, and J. C. Martinou.** 1999. Bid-induced conformational change of Bax is responsible for mitochondrial cytochrome c release during apoptosis. J Cell Biol **144:**891-901.

12. **Estaquier, J., T. Idziorek, F. de Bels, F. Barre-Sinoussi, B. Hurtrel, A. M. Aubertin, A. Venet, M. Mehtali, E. Muchmore, P. Michel, and et al.** 1994. Programmed cell death and AIDS: significance of T-cell apoptosis in pathogenic and nonpathogenic primate lentiviral infections. Proc Natl Acad Sci U S A **91:**9431-5.

13. **Green, D. R., and G. Kroemer.** 2004. The pathophysiology of mitochondrial cell death. Science **305:**626-9.

14. **Gross, A., J. Jockel, M. C. Wei, and S. J. Korsmeyer.** 1998. Enforced dimerization of BAX results in its translocation, mitochondrial dysfunction and apoptosis. Embo J **17:**3878-85.

15. **Gross, A., J. M. McDonnell, and S. J. Korsmeyer.** 1999. BCL-2 family members and the mitochondria in apoptosis. Genes Dev **13:**1899-911.

16. **Hofman, P., and P. Auberger.** 2000. [Roles and mechanisms of apoptosis in infectious diseases]. Ann Pathol **20:**313-22.

17. **Holloway, G., and B. S. Coulson.** 2006. Rotavirus Activates JNK and p38 Signaling Pathways in Intestinal Cells, Leading to AP-1-Driven Transcriptional Responses and Enhanced Virus Replication. J Virol **80:**10624-33.

18. **Hsu, Y. T., and R. J. Youle.** 1998. Bax in murine thymus is a soluble monomeric protein that displays differential detergent-induced conformations. J Biol Chem **273:**10777-83.

19. **Hsu, Y. T., and R. J. Youle.** 1997. Nonionic detergents induce dimerization among members of the Bcl-2 family. J Biol Chem **272:**13829-34.

20. **Jin, Z., and W. S. El-Deiry.** 2005. Overview of cell death signaling pathways. Cancer Biol Ther **4:**139-63.

21. **Kim, B. J., S. W. Ryu, and B. J. Song.** 2006. JNK- and p38 kinase-mediated phosphorylation of Bax leads to its activation and mitochondrial translocation and to apoptosis of human hepatoma HepG2 cells. J Biol Chem **281:**21256-65.

22. **Kominsky, D. J., R. J. Bickel, and K. L. Tyler.** 2002. Reovirus-induced apoptosis requires mitochondrial release of Smac/DIABLO and involves reduction of cellular inhibitor of apoptosis protein levels. J Virol **76:**11414-24.

476 23. **Korsmeyer, S. J., M. C. Wei, M. Saito, S. Weiler, K. J. Oh, and P. H. Schlesinger.**
477 2000. Pro-apoptotic cascade activates BID, which oligomerizes BAK or BAX into
478 pores that result in the release of cytochrome c. Cell Death Differ **7:**1166-73.
479 24. **Kuwana, T., L. Bouchier-Hayes, J. E. Chipuk, C. Bonzon, B. A. Sullivan, D. R.**
480 **Green, and D. D. Newmeyer.** 2005. BH3 domains of BH3-only proteins
481 differentially regulate Bax-mediated mitochondrial membrane permeabilization both
482 directly and indirectly. Mol Cell **17:**525-35.
483 25. **Letai, A., M. C. Bassik, L. D. Walensky, M. D. Sorcinelli, S. Weiler, and S. J.**
484 **Korsmeyer.** 2002. Distinct BH3 domains either sensitize or activate mitochondrial
485 apoptosis, serving as prototype cancer therapeutics. Cancer Cell **2:**183-92.
486 26. **Li, H., H. Zhu, C. J. Xu, and J. Yuan.** 1998. Cleavage of BID by caspase 8 mediates
487 the mitochondrial damage in the Fas pathway of apoptosis. Cell **94:**491-501.
488 27. **Li, S., Y. Zhao, X. He, T. H. Kim, D. K. Kuharsky, H. Rabinowich, J. Chen, C.**
489 **Du, and X. M. Yin.** 2002. Relief of extrinsic pathway inhibition by the Bid-dependent
490 mitochondrial release of Smac in Fas-mediated hepatocyte apoptosis. J Biol Chem
491 **277:**26912-20.
492 28. **Liu, Y., Y. Pu, and X. Zhang.** 2006. Role of the mitochondrial signaling pathway in
493 murine coronavirus-induced oligodendrocyte apoptosis. J Virol **80:**395-403.
494 29. **Lundgren, O., and L. Svensson.** 2001. Pathogenesis of rotavirus diarrhea. Microbes
495 Infect **3:**1145-56.
496 30. **Luo, X., I. Budihardjo, H. Zou, C. Slaughter, and X. Wang.** 1998. Bid, a Bcl2
497 interacting protein, mediates cytochrome c release from mitochondria in response to
498 activation of cell surface death receptors. Cell **94:**481-90.

31. **Michelangeli, F., M. C. Ruiz, J. R. del Castillo, J. E. Ludert, and F. Liprandi.** 1991. Effect of rotavirus infection on intracellular calcium homeostasis in cultured cells. Virology **181:**520-7.

32. **Morris, A. P., and M. K. Estes.** 2001. Microbes and microbial toxins: paradigms for microbial-mucosal interactions. VIII. Pathological consequences of rotavirus infection and its enterotoxin. Am J Physiol Gastrointest Liver Physiol **281:**G303-10.

33. **Murphy, K. M., U. N. Streips, and R. B. Lock.** 2000. Bcl-2 inhibits a Fas-induced conformational change in the Bax N terminus and Bax mitochondrial translocation. J Biol Chem **275:**17225-8.

34. **Muzio, M., A. M. Chinnaiyan, F. C. Kischkel, K. O'Rourke, A. Shevchenko, J. Ni, C. Scaffidi, J. D. Bretz, M. Zhang, R. Gentz, M. Mann, P. H. Krammer, M. E. Peter, and V. M. Dixit.** 1996. FLICE, a novel FADD-homologous ICE/CED-3-like protease, is recruited to the CD95 (Fas/APO-1) death--inducing signaling complex. Cell **85:**817-27.

35. **Narita, M., S. Shimizu, T. Ito, T. Chittenden, R. J. Lutz, H. Matsuda, and Y. Tsujimoto.** 1998. Bax interacts with the permeability transition pore to induce permeability transition and cytochrome c release in isolated mitochondria. Proc Natl Acad Sci U S A **95:**14681-6.

36. **Natoni, A., G. E. Kass, M. J. Carter, and L. O. Roberts.** 2006. The mitochondrial pathway of apoptosis is triggered during feline calicivirus infection. J Gen Virol **87:**357-61.

37. **Nutt, L. K., A. Pataer, J. Pahler, B. Fang, J. Roth, D. J. McConkey, and S. G. Swisher.** 2002. Bax and Bak promote apoptosis by modulating endoplasmic reticular and mitochondrial Ca2+ stores. J Biol Chem **277:**9219-25.

523 38. **Oltvai, Z. N., C. L. Milliman, and S. J. Korsmeyer.** 1993. Bcl-2 heterodimerizes in
524 vivo with a conserved homolog, Bax, that accelerates programmed cell death. Cell
525 **74:**609-19.
526 39. **Pan, Z., M. B. Bhat, A. L. Nieminen, and J. Ma.** 2001. Synergistic movements of
527 Ca(2+) and Bax in cells undergoing apoptosis. J Biol Chem **276:**32257-63.
528 40. **Parashar, U. D., C. J. Gibson, J. S. Bresse, and R. I. Glass.** 2006. Rotavirus and
529 severe childhood diarrhea. Emerg Infect Dis **12:**304-6.
530 41. **Pinton, P., and R. Rizzuto.** 2006. Bcl-2 and Ca2+ homeostasis in the endoplasmic
531 reticulum. Cell Death Differ **13:**1409-18.
532 42. **Puthalakath, H., and A. Strasser.** 2002. Keeping killers on a tight leash:
533 transcriptional and post-translational control of the pro-apoptotic activity of BH3-only
534 proteins. Cell Death Differ **9:**505-12.
535 43. **Ramig, R. F.** 2004. Pathogenesis of intestinal and systemic rotavirus infection. J Virol
536 **78:**10213-20.
537 44. **Reed, J. C.** 1998. Bcl-2 family proteins. Oncogene **17:**3225-36.
538 45. **Roulston, A., R. C. Marcellus, and P. E. Branton.** 1999. Viruses and apoptosis.
539 Annu Rev Microbiol **53:**577-628.
540 46. **Ruiz, M. C., J. Cohen, and F. Michelangeli.** 2000. Role of Ca2+in the replication
541 and pathogenesis of rotavirus and other viral infections. Cell Calcium **28:**137-49.
542 47. **Superti, F., M. G. Ammendolia, A. Tinari, B. Bucci, A. M. Giammarioli, G.**
543 **Rainaldi, R. Rivabene, and G. Donelli.** 1996. Induction of apoptosis in HT-29 cells
544 infected with SA-11 rotavirus. J Med Virol **50:**325-34.
545 48. **Tian, P., M. K. Estes, Y. Hu, J. M. Ball, C. Q. Zeng, and W. P. Schilling.** 1995.
546 The rotavirus nonstructural glycoprotein NSP4 mobilizes Ca2+ from the endoplasmic
547 reticulum. J Virol **69:**5763-72.

548 49. **Tsuruta, F., J. Sunayama, Y. Mori, S. Hattori, S. Shimizu, Y. Tsujimoto, K.**
549 **Yoshioka, N. Masuyama, and Y. Gotoh.** 2004. JNK promotes Bax translocation to
550 mitochondria through phosphorylation of 14-3-3 proteins. Embo J **23:**1889-99.
551 50. **van Loo, G., X. Saelens, M. van Gurp, M. MacFarlane, S. J. Martin, and P.**
552 **Vandenabeele.** 2002. The role of mitochondrial factors in apoptosis: a Russian
553 roulette with more than one bullet. Cell Death Differ **9:**1031-42.
554 51. **Vaux, D. L., and S. J. Korsmeyer.** 1999. Cell death in development. Cell **96:**245-54.
555 52. **Wang, X.** 2001. The expanding role of mitochondria in apoptosis. Genes Dev
556 **15:**2922-33.
557 53. **Wei, M. C., W. X. Zong, E. H. Cheng, T. Lindsten, V. Panoutsakopoulou, A. J.**
558 **Ross, K. A. Roth, G. R. MacGregor, C. B. Thompson, and S. J. Korsmeyer.** 2001.
559 Proapoptotic BAX and BAK: a requisite gateway to mitochondrial dysfunction and
560 death. Science **292:**727-30.
561 54. **Wolter, K. G., Y. T. Hsu, C. L. Smith, A. Nechushtan, X. G. Xi, and R. J. Youle.**
562 1997. Movement of Bax from the cytosol to mitochondria during apoptosis. J Cell
563 Biol **139:**1281-92.
564 55. **Xu, A., A. R. Bellamy, and J. A. Taylor.** 1998. BiP (GRP78) and endoplasmin
565 (GRP94) are induced following rotavirus infection and bind transiently to an
566 endoplasmic reticulum-localized virion component. J Virol **72:**9865-72.

FIGURE LEGENDS

Fig. 1. RRV induces apoptosis in MA104 cells.

A. DNA-fragmentation in RRV-infected MA104 cells. At the indicated times post-infection, DNA fragmentation was analyzed using the Cell Death Detection ELISA^{PLUS} assay which detects the appearance of histone-associated low molecular weight DNA in the cytoplasm of cells. Mock-infected and staurosporine (STS)-treated MA104 cells were used as negative and positive controls, respectively. Enrichment Factor was calculated as the absorbance at 405/492 nm for treated cells divided by that of the corresponding untreated cells. Data are means ± S.D. of three experiments. *$P<0.05$ by Student t-test comparing RRV-infected MA104 cells to mock-infected MA104 cells.

B. RRV infection triggered caspase-3 activation and PARP processing in MA104 cells. At the indicated times post-infection, whole cell extracts were subjected to western blot analysis with anti-caspase-3 and anti-PARP antibodies. Mock-infected MA104 cells were used as negative controls. An asterisk (*) indicates a nonspecific protein band which was used as a protein loading control. Positions of markers of molecular weight are indicated at the left of panel.

C. RRV-induced apoptosis is dependent on caspases activation in MA104 cells. MA104 cells were treated or non-treated with the broad caspase inhibitor z-VAD-fmk (10 μM), the specific caspase-9 inhibitor z-LEHD-fmk (10 μM) or the specific caspase-3 inhibitor z-DEVD-fmk (10 μM) 2 h before RRV infection and maintained throughout the infection. Mock- and RRV-infected MA104 cells were analyzed 14 h post-infection (p.i) by flow cytometry after acridine orange nuclear dye staining and the fold increase of apoptosis was calculated as the ratio of the apoptotic cell percentages for RRV-infected MA104 cells to that for mock-infected MA104 cells. Data are expressed as means of three independent experiments. Error bars

represent the standard errors of the mean, *P<0.05 by Student t-test comparing non-treated MA104 cells to treated MA104 cells.

Fig. 2. Mitochondrial apoptotic pathway is activated in RRV-infected MA104 cells.
Time course of cytochrome c and Smac/Diablo release in RRV-infected MA104 cells. At the indicated times post-infection, cells were collected and subjected to subcellular fractionation as described in Material and Methods. The cytosolic (C) and heavy membrane (HM) fraction proteins were assayed by western blot analysis for cytochrome c and Smac/Diablo. Mock-infected MA104 cells were used as negative controls. Cox IV and tubulin were used as protein loading controls for heavy membrane and cytosolic fractions, respectively. Positions of markers of molecular weight are indicated at the left of panel. Cytochrome c and Smac/Diablo protein levels of heavy membrane and cytosolic fractions were determined by densitometry and plotted as ratios relative to the levels of Cox IV and tubulin, respectively (*lower panel*).

Fig. 3. RRV induces caspase-8 activation and Bid processing in MA104 cells.
A. Time course of caspase-8 activation and Bid processing in RRV-infected MA104 cells. At the indicated times post-infection, whole cell extracts were subjected to immunoblot analysis with anti-caspase-8 and anti-Bid antibodies. Mock-infected MA104 cells were used as negative controls. Tubulin was used as a control for protein loading. Positions of markers of molecular weight are indicated at the left of panel. Bid protein levels were determined by densitometry and plotted as ratios relative to the levels of tubulin (*lower panel*).
B. Caspase-8 activation was determined in mock- and RRV-infected MA104 cells (14 h p.i.) by flow cytometry using cell-permeable, fluorescein-labeled inhibitor (FAM-LETD-fmk), that binds specifically on active caspase-8, as described in Material and Methods. Histogram

representative of two independent experiments is shown. The percentage of cells positive for activated caspase-8 following RRV infection is indicated.

Fig. 4. Cytochrome c release in RRV-infected MA104 cells is caspase-independent.

A. The broad-spectrum caspase inhibitor z-VAD-fmk inhibits Bid and PARP processing in RRV-infected MA104 cells. Mock- and RRV-infected MA104 cells were pretreated or not pretreated with 100 μM z-VAD-fmk for 2 h before and during RRV infection. Whole cell extracts were prepared 14 h post-infection and Bid and PARP were assayed by western blot analysis. Mock-infected MA104 cells were used as negative controls. Tubulin was used as a control for protein loading. Positions of markers of molecular weight are indicated at the left of panel.

B. z-VAD-fmk did not inhibit cytochrome c release in RRV-infected MA104 cells. Mock- and RRV-infected MA104 cells were pretreated or not pretreated with 100 μM z-VAD-fmk for 2 h before and during infection. Fourteen hours after RRV infection, the cytosolic and heavy membrane fractions were assayed for cytochrome c by western blotting. Mock-infected MA104 cells were used as negative controls, Cox IV and tubulin were used as protein loading controls for heavy membrane and cytosolic fractions, respectively. Positions of markers of molecular weight are indicated at the left of panel.

Fig. 5. RRV induces Bax protein activation in MA104 cells.

A. RRV induced Bax conformational change in MA104 cells. At the indicated time post-infection (p.i), MA104 cells were lysed in immunoprecipitation buffer containing the zwitterionic detergent Chaps (which maintains Bax in its activated conformation). Anti-Bax 6A7 antibody was used to immunoprecipitate conformationally active Bax protein. The immunoprecipitates were analyzed by immunoblotting with anti-Bax antibody.

Immunoglobulin light chains are indicated with an asterisk (*). Mock-infected MA104 cells were used as negative control. Positions of markers of molecular weight are indicated at the left of panel.

B. z-VAD-fmk did not inhibit Bax conformational change in RRV-infected MA104 cells. RRV-infected MA104 cells were pretreated or not pretreated with 100 μM z-VAD-fmk for 2 h before and during infection. Whole cell lysates were immunoprecipitated with activated Bax antibody (clone 6A7) and then analyzed by immunoblotting with anti-Bax antibody. Mock-infected MA104 cells were used as negative control. Immunoglobulin light chains are indicated with an asterisk (*). Positions of markers of molecular weight are indicated at the left of panel.

C. RRV infection promoted Bcl-2 degradation in MA104 cells. At the indicated times post-infection, whole cell lysates were prepared. Bax and Bcl-2 proteins were detected by western blotting with anti-Bax and anti-Bcl-2 specific antibodies. Mock-infected MA104 cells were used as negative controls. Tubulin was used as a control for protein loading. Positions of markers of molecular weight are indicated at the left of panel.

Fig. 6. Cytochrome c release induced by RRV infection of MA104 cells is Bax-dependent.

A. Knock down of Bax expression in MA104 cells. Cells were transfected with specific Bax siRNA or irrelevant siRNA. Bax protein was then assayed in whole cell lysates from by immunoblotting. Levels of tubulin were used as protein loading controls (*upper panel*). Bax protein levels were determined by densitometry and plotted as ratios relative to the levels of tubulin. Positions of markers of molecular weight are indicated at the left of panel. The graph shows the mean percentage of Bax expression inhibition in three independent experiments. Error bars represent the standard errors of the mean, *$P<0.05$ by Student t-test comparing

667 irrelevant siRNA-transfected to Bax siRNA-transfected MA104 cells (*lower panel*).

668 **B.** siRNA-induced silencing of the Bax gene results in reduction of RRV-induced cytochrome
669 c release in MA104 cells. Cells were infected with RRV 48 h post-transfection and
670 cytochrome c was analyzed in cytosolic (C) and heavy membrane fractions (M) by western
671 blotting 14h post-infection. Mock-infected MA104 cells were used as negative controls.
672 Tubulin and Cox IV were used as controls for protein loading of cytosolic (C) and heavy
673 membrane (M) fractions, respectively. Positions of markers of molecular weight are indicated
674 at the left of panel. Cytochrome c protein levels of heavy membrane and cytosolic fractions
675 were determined by densitometry and plotted as ratios relative to the levels of Cox IV and
676 tubulin, respectively (*lower panel*).

677 **C.** siRNA-induced silencing of the Bax gene results in reduction of RRV-induced apoptosis in
678 MA104 cells. Cells were infected with RRV 48 h post-transfection and the percentage of
679 apoptosis was determined by flow cytometry after Acridine Orange (AO) staining. MA104
680 cells transfected with irrelevant siRNA was used as negative control.

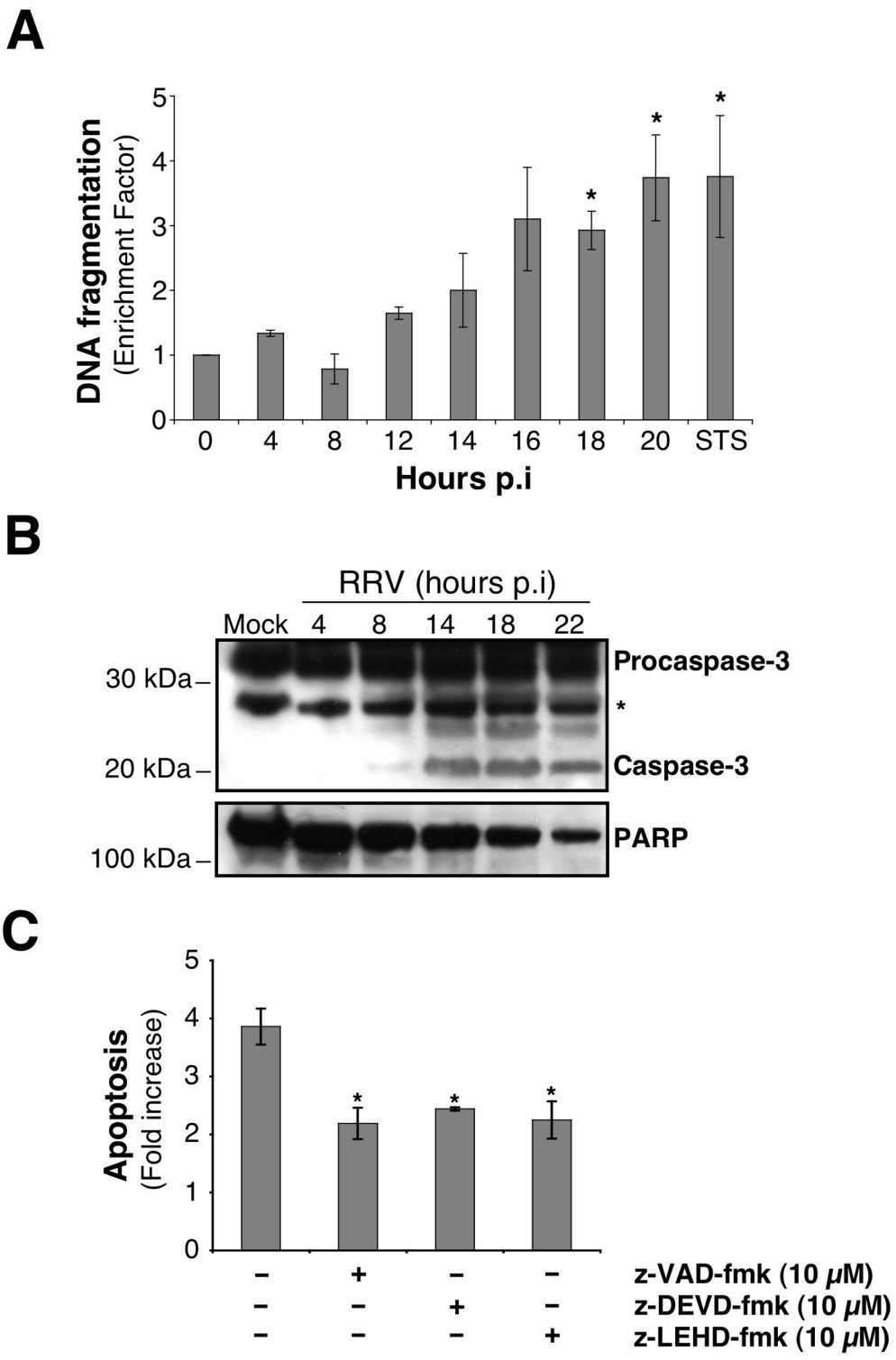

A
DNA fragmentation
(Enrichment Factor)
0
1
2
3
4
5
0
4
8
12
14
16
18
20
STS
Hours p.i
B
RRV (hours p.i)
Mock
4
8
14
18
22
30 kDa
20 kDa
100 kDa
Procaspase-3
*
Caspase-3
PARP
C
Apoptosis
(Fold increase)
0
1
2
3
4
5
z-VAD-fmk (10 μM)
z-DEVD-fmk (10 μM)
z-LEHD-fmk (10 μM)

Figure 1

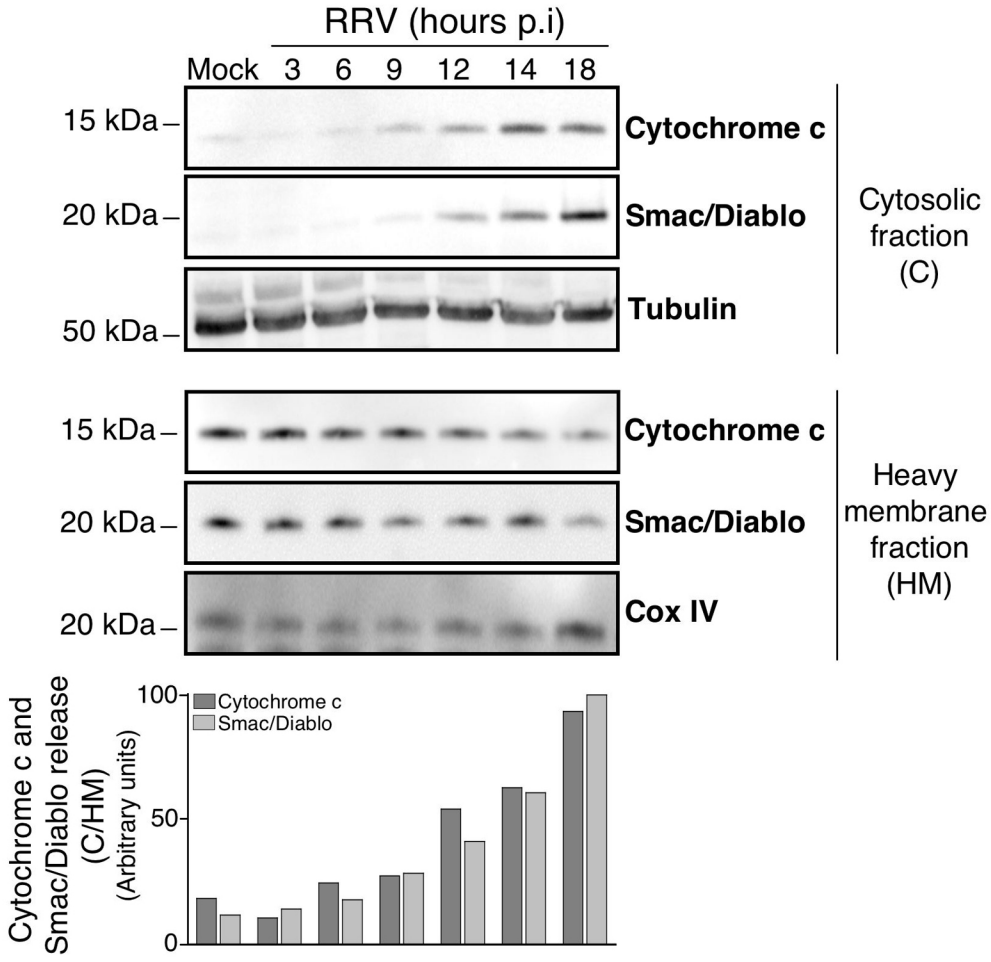

RRV (hours p.i)
Mock 3 6 9 12 14 18
15 kDa
Cytochrome c
20 kDa
Smac/Diablo
Tubulin
50 kDa
Cytosolic fraction (C)
15 kDa
Cytochrome c
20 kDa
Smac/Diablo
20 kDa
Cox IV
Heavy membrane fraction (HM)
Cytochrome c and Smac/Diablo release (C/HM) (Arbitrary units)
100
50
0
Cytochrome c
Smac/Diablo

Figure 2

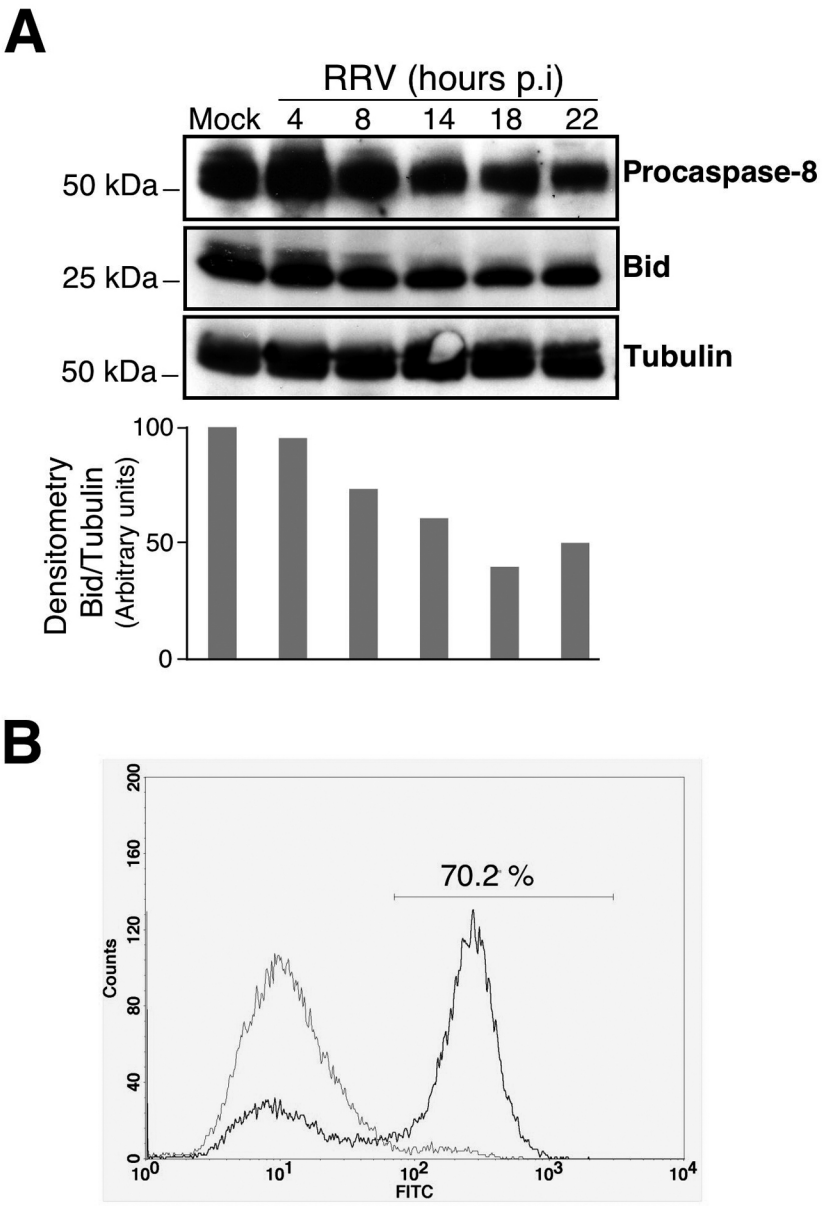

A
RRV (hours p.i)
Mock
4
8
14
18
22
50 kDa
Procaspase-8
25 kDa
Bid
50 kDa
Tubulin
Densitometry
Bid/Tubulin
(Arbitrary units)
100
50
0
B
70.2 %
Counts
200
160
120
80
40
0
10^0
10^1
10^2
10^3
10^4
FITC

Figure 3

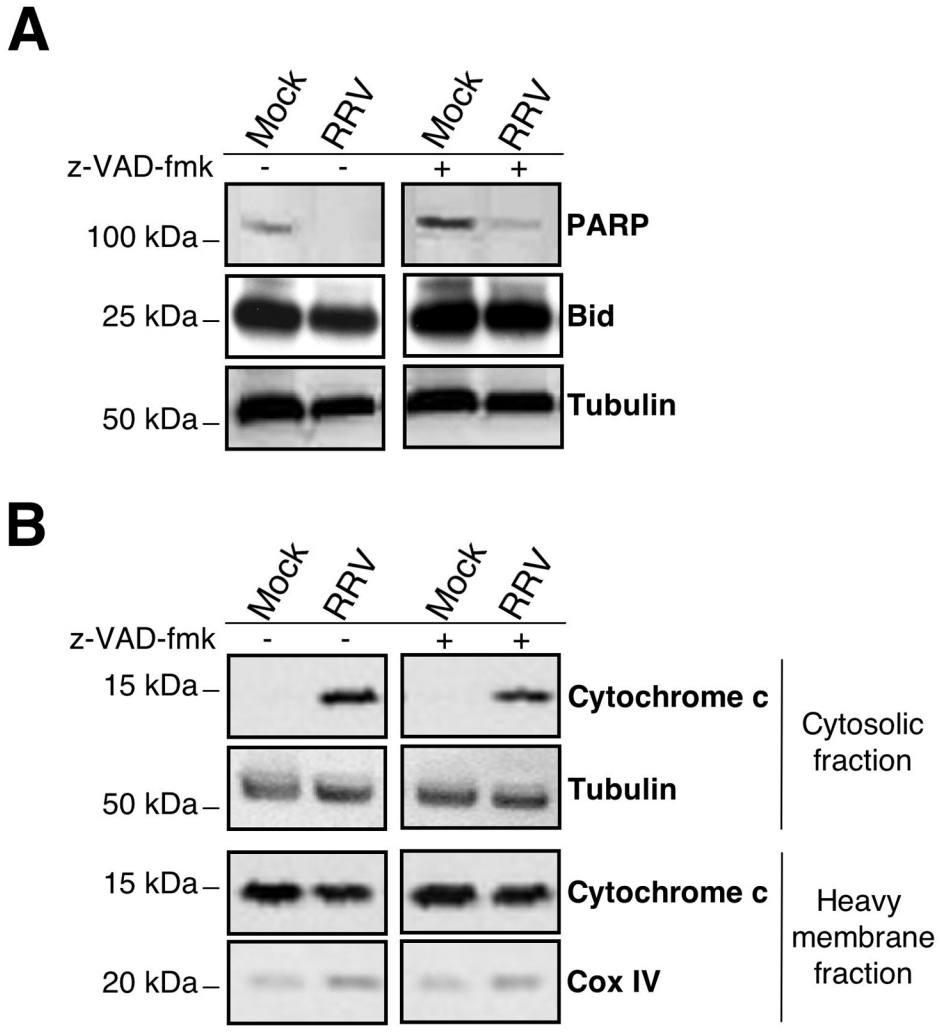

A
Mock
RRV
Mock
RRV
z-VAD-fmk
-
-
+
+
100 kDa
PARP
25 kDa
Bid
50 kDa
Tubulin
B
Mock
RRV
Mock
RRV
z-VAD-fmk
-
-
+
+
15 kDa
Cytochrome c
50 kDa
Tubulin
Cytosolic fraction
15 kDa
Cytochrome c
20 kDa
Cox IV
Heavy membrane fraction

Figure 4

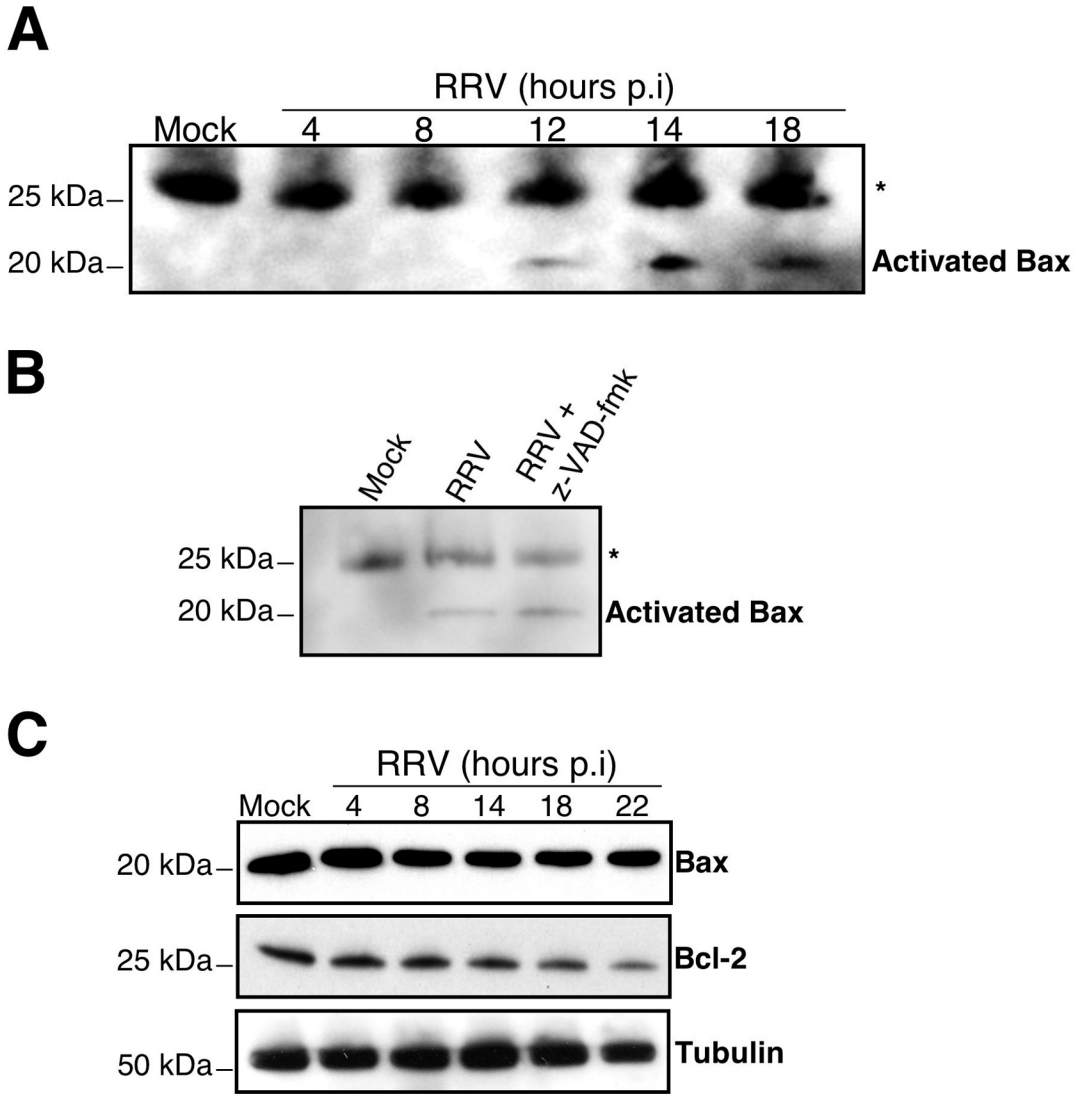

A
RRV (hours p.i)
Mock
4
8
12
14
18
25 kDa
20 kDa
*
Activated Bax
B
Mock
RRV
RRV +
z-VAD-fmk
25 kDa
20 kDa
*
Activated Bax
C
RRV (hours p.i)
Mock
4
8
14
18
22
20 kDa
Bax
25 kDa
Bcl-2
50 kDa
Tubulin

Figure 5

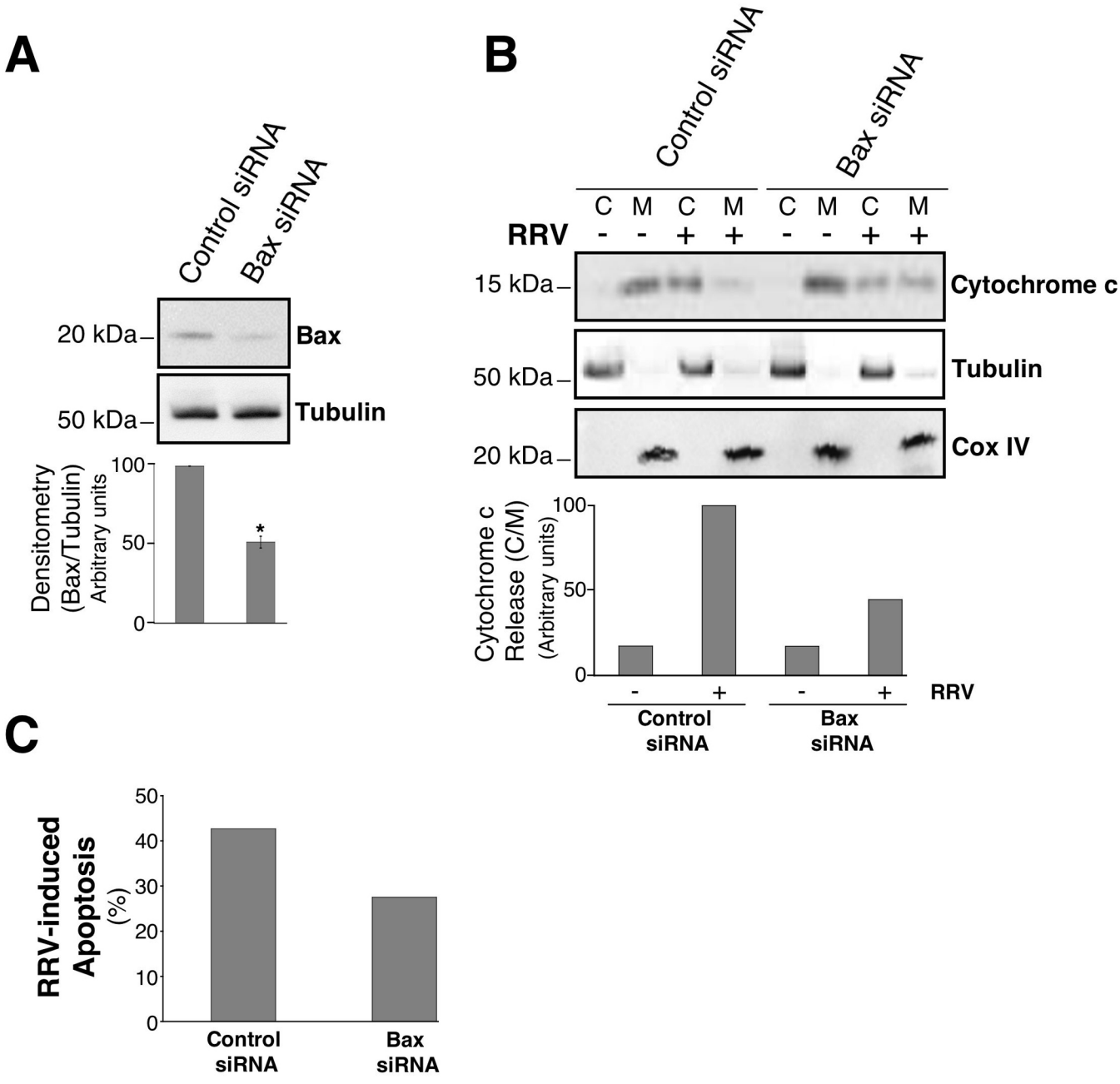

A
Control siRNA
Bax siRNA
20 kDa
Bax
50 kDa
Tubulin
Densitometry (Bax/Tubulin) Arbitrary units
100
50
0
*
B
Control siRNA
Bax siRNA
C M C M C M C M
RRV - - + + - - + +
15 kDa
Cytochrome c
50 kDa
Tubulin
20 kDa
Cox IV
Cytochrome c Release (C/M) (Arbitrary units)
100
50
0
- + - +
RRV
Control siRNA
Bax siRNA
C
RRV-induced Apoptosis (%)
50
40
30
20
10
0
Control siRNA
Bax siRNA

Figure 6